Coherent Kondo-lattice state and the crossover transitions in the Anderson-lattice model

H. Kaga, H. Kubo, and T. Fujiwara
Department of Physics, Niigata University, Niigata 950-21, Japan
(Received 19 March 1987)

We study the formation of the coherent Kondo-lattice state responsible for the heavy-fermion quasiparticle state in the Anderson-lattice model, and discuss the crossover transitions between the incoherent and coherent Kondo-lattice states, and between the coherent Kondo-lattice state and the valence-fluctuation state. The f-electron lattice Green function is obtained in the self-consistent equation-of-motion method in the decoupling approximation, and is found to have a characteristic feature of lattice different from the impurity Green function. The overall f-electron densities of states are studied as a function of temperature. In the Kondo-lattice regime, as temperature decreases, the crossover transition from the incoherent to the coherent Kondo-lattice states takes place before the single-site Kondo resonances are fully developed at individual sites. Thus the lattice Kondo effect is distinct from the impurity one. The coherent Kondo-lattice state, which has a sharp pseudogap at the Fermi level, fully develops at the coherence temperature $T_0 \sim 0.1 T_K$, which is in agreement with the experimental results.

I. INTRODUCTION

The heavy-fermion state[1,2] found in Ce compounds $CeAl_3$, $CeCu_2Si_2$, $CeCu_6$, and some uranium compounds is arousing a considerable interest in the circle of condensed-matter physicists. The study of this subject[1] may be related to the fundamental problems such as the development of coherence in the Kondo effect,[3] its competition with the Ruderman-Kittel-Kasuya-Yosida (RKKY) interaction,[3,4] and the mechanism[5] for the unusual heavy-fermion superconductivity of $CeCu_2Si_2$,[6] UBe_{13},[7] and UPt_3.[8]

Resistivity measurements of $CeAl_3$,[9,10] $CeCu_2Si_2$,[11] and $CeCu_6$,[12] show that at high temperatures these systems behave like an independent-impurity Kondo system with an approximate logarithmic temperature dependence, and at low temperatures they assume a coherent Fermi-liquid state with a T^2 temperature dependence after a resistivity maximum in the intermediate temperature range of some tens Kelvins. The low-temperature specific heats $C(T)$ of these systems, $CeAl_3$,[13,9,14] $CeCu_2Si_2$,[13] and $CeCu_6$,[15] indicate an enormous enhancement (of order $\sim 10^3$) in the specific-heat coefficient $\gamma(T)=C(T)/T$ as large as 1–2 J/mol K^2, suggesting a very heavy effective mass m^* for the Fermi-liquid state; hence the name heavy-fermion state. Furthermore, the observed temperature dependences of $\gamma(T)$ for all the heavy-fermion Ce compounds show a peak $\gamma_{\max}$ at the characteristic temperature T_0 (~ 0.5 K), called the coherence temperature, and a sharp decrease at lower temperatures. These coherence temperatures[13–15] T_0 found from $\gamma_{\max}=\gamma(T_0)$ approximately coincide with the coherence temperatures T_0 below which the T^2 dependence of the resistivity,[9–12] which is expected in the coherent Fermi liquid, is observed, and are on an order of magnitude smaller than the impurity Kondo temperature T_K.

These behaviors of $\gamma(T)$ around the coherence temperature T_0 have been interpreted by Bredl *et al.*[13] as the effect of a pseudogap that may be formed at the Fermi level due to the development of coherence between the individual-site Kondo resonances. The possibility of such a pseudogap in the Kondo resonance of the Anderson-lattice model which was suggested by Martin[16] has been first shown by Grewe[17] in the calculations of f-electron density of states. The crossover transition from the incoherent to the coherent lattice Kondo states with decrease in temperature has been recently investigated by Lacroix[18] in the Kondo-lattice model by a functional-integral method, and by Koyama and Tachiki[19] in the Anderson-lattice model by a perturbation theory of the one-loop approximation of spin fluctuation. While a pseudogap is found in the coherent Kondo state of the former, no pseudogap is formed in the latter showing a sharp heavy-fermion peak at the Fermi energy ϵ_F. Therefore, the existence of the pseudogap and the position of the coherent Kondo peak with respect to the Fermi energy are not well understood yet. Furthermore, the precise interpretation of the coherence temperature T_0 and its relation to the Kondo temperature T_K are still unclear. These problems should be investigated in a more systematic treatment of the various Kondo-lattice states, including those in the border with the valence-fluctuation states.

In this paper we study the lattice Kondo resonance in the Anderson-lattice model in comparison to the impurity Kondo resonance in the self-consistent equation-of-motion method by Green-function decoupling approximation. We make the unified treatments of both the Kondo-lattice system and the valence-fluctuation system by calculating the temperature-dependent f-electron densities of states. However, we do not take into account here the RKKY interaction derived from the intersite interactions. This effect can, in principle, be treated in the higher-stage decoupling approximation,

but it would be awfully complicated to solve the resulting self-consistent integral equations. The inclusion of the RKKY effect in the study of the lattice Kondo effect is important, as has been shown recently by Abrahams and Varma[20] and Jones and Varma[21] because, in addition to the competition between the two effects, the realizable ground states are the modified ones; the spatially correlated (or coherent) Kondo state and the reduced-moment magnetic state. We will demonstrate that as temperature decreases, the Kondo-lattice system exhibits the two crossover transitions in the f-electron densities of states $\rho_f(\omega)$ near the Fermi energy ϵ_F; i.e., the first one to the impuritylike incoherent Kondo-resonance states, and the second one to the coherent Kondo-lattice states with a pseudogap, completing, respectively, at about several T_K and $0.1T_K$. The coherent Kondo-lattice resonance is responsible for the heavy-fermion quasiparticle state. The transition from the coherent Kondo-lattice (heavy-fermion) states to the valence-fluctuation states with approach of the f-level ε_f to the Fermi level ϵ_F takes place also in a continuous crossover fashion, where a sharp coherent Kondo-resonance spike and a pseudogap are swept away to become a double-peak resonance above ϵ_F.

Theumann[22] and Lacroix[23] have studied the impurity Anderson model in the Green-function decoupling approximation of Nagaoka,[24] and Lacroix[23] has shown that in the Kondo limit the Kondo-resonance peak of width T_K arises at the Fermi-level ϵ_F in the f-electron density of states. The Anderson-lattice model has been recently studied extensively by the decoupling approximations.[25–28] In the Kondo-lattice regime only the impuritylike Kondo resonance has been so far obtained,[25,26] and no characteristic features of the periodic system such as a coherent Kondo resonance and pseudogap have been reported.[25–27]

Recently, there have been active studies on the residual interactions between heavy fermions, i.e., quasiparticles formed at the low temperatures in the Anderson-lattice model by Tesanovic and Valls[29] and by Lavagna *et al.*[30] and in the Kondo-lattice model by Auerbach and Levin.[31] These studies are important because the remaining quasiparticle interactions determine the low-temperature properties of the system. A superconducting instability may be induced if the pairing interaction is dominant,[30,29] and the type of the superconducting state can be investigated from its vertex.[30] By connecting the self-energy and vertex of the residual interaction with the Landau Fermi-liquid parameters the low-temperature heavy-fermion properties in the coherent states are successfully derived.[31] All these interactions are derived around the mean-field coherent states obtained either by the equation-of-motion method[29] or by the functional-integral method,[30,31] which are applied to the slave-boson Hamiltonian[29,30] of the Anderson lattice and to the Kondo-boson version[31] of the Kondo lattice. Therefore, these coherent ground states are realized by a phase transition from the high-temperature phase. Thus, this is a contrasting feature different from our result that the coherent state is reached by the two crossover transitions because fluctuations beyond a mean-field approximation are partly incorporated in the decoupling approximation. However, the remaining effective interactions are not explicitly evaluated in this paper.

In Sec. II the Green functions of localized f and conduction electrons for the Anderson-lattice model are derived by the self-consistent decoupling approximation in the equations of motion. The f-electron Green function of the Anderson-lattice model is compared with those of the impurity Anderson model and of the single-site approximation of the lattice. The lattice f-electron Green function and thus the self-energy in the present treatment are found to have a characteristic form due to lattice periodicity, different from the other two. The use of the impurity self-energy in the lattice Green function which is sometimes made[17,32,33] is pointed out to lead to the incorrect results at low temperatures. In Sec. III the characteristic temperatures for the f-electron density of states near the Fermi energy ϵ_F are explored both in the impurity and the lattice systems in the Kondo limit. The impurity system including the orbital-degenerate case is found to have the onset temperature T_K' and the developed-resonance temperature T_K for the impurity Kondo resonance. In the Kondo-lattice system, however, we show that even with the same onset temperature T_K', the impuritylike incoherent Kondo resonance crosses over to the coherent Kondo-lattice resonance above T_K (at several T_K). When the crossover is completed at the coherence temperature $T_0 \sim 0.1\ T_K$, a coherence is fully developed and the heavy-fermion quasiparticle picture becomes valid. In Sec. IV the f-electron spectra of the impurity and lattice Kondo resonances are calculated numerically for the same parameters in the limit of the infinite Coulomb repulsion U as a function of temperature. The valence-fluctuation regime of the Anderson lattice is also studied. Discussions are given in Sec. V.

II. MODEL AND LATTICE GREEN FUNCTION

A. Self-consistent Green-function decoupling approximation

Except in Sec. III where the characteristic temperatures are studied, we treat the Anderson-lattice model without orbital degeneracy which is the periodic version of the impurity Anderson model,[34]

$$H=\sum_{\mathbf{k},\sigma}\varepsilon_{\mathbf{k}}d^{\dagger}_{\mathbf{k},\sigma}d_{\mathbf{k},\sigma}+\varepsilon_f\sum_{i,\sigma}f^{\dagger}_{i,\sigma}f_{i,\sigma}+U\sum_i f^{\dagger}_{i,\uparrow}f^{\dagger}_{i,\downarrow}f_{i,\downarrow}f_{i,\uparrow}+\frac{V}{\sqrt{N}}\sum_{i,\mathbf{k},\sigma}(e^{i\mathbf{k}\cdot\mathbf{R}_i}d^{\dagger}_{\mathbf{k},\sigma}f_{i,\sigma}+e^{-i\mathbf{k}\cdot\mathbf{R}_i}f^{\dagger}_{i,\sigma}d_{\mathbf{k},\sigma}), \quad (1)$$

where $\varepsilon_{\mathbf{k}}$ is the conduction band ($-D\le\varepsilon_{\mathbf{k}}\le D$) whose density of states is assumed to be constant $\rho=1/2D$, ε_f is the f-electron level, U the Coulomb repulsion between f electrons with opposite spins on the same site, and V the hybridization mixing between f and conduction electrons, which are represented by the creation operators $f^{\dagger}_{i,\sigma}$ and $d^{\dagger}_{\mathbf{k},\sigma}$, respectively.

We set up the equation of motion for the f-electron

retarded Green function $\langle\langle f_{i,\sigma}, f^{\dagger}_{j,\sigma}\rangle\rangle$ (compare with the impurity one in Ref. 23),

$$\left[\omega=\varepsilon_f-\frac{V^2}{\omega-\varepsilon_{\mathbf{k}}}\right]\sum_i e^{i\mathbf{k}\cdot\mathbf{R}_i}\langle\langle f_{i,\sigma}, f^{\dagger}_{j,\sigma}\rangle\rangle = e^{i\mathbf{k}\cdot\mathbf{R}_j}+U\sum_i e^{i\mathbf{k}\cdot\mathbf{R}_i}\langle\langle f_{i,\sigma}n_{i,-\sigma}, f^{\dagger}_{j,\sigma}\rangle\rangle \ . \tag{2}$$

The two-particle Green function

$$\langle\langle f_{i,\sigma}n_{i,-\sigma}, f^{\dagger}_{j,\sigma}\rangle\rangle$$

that appears on the right-hand side of Eq. (2) satisfies the equation of motion,

$$\begin{aligned}(\omega-\varepsilon_f-U)\langle\langle f_{i,\sigma}n_{i,-\sigma}, f^{\dagger}_{j,\sigma}\rangle\rangle &= \langle n_{i,-\sigma}\rangle\delta_{ij}+\frac{V}{\sqrt{N}}\sum_{\mathbf{k}} e^{-i\mathbf{k}\cdot\mathbf{R}_i}\langle\langle d_{\mathbf{k},\sigma}n_{i,-\sigma}, f^{\dagger}_{j,\sigma}\rangle\rangle-\frac{V}{\sqrt{N}}\sum_{\mathbf{k}} e^{-i\mathbf{k}\cdot\mathbf{R}_i}\langle\langle d_{\mathbf{k},-\sigma}f^{\dagger}_{i,-\sigma}f_{i,\sigma}, f^{\dagger}_{j,\sigma}\rangle\rangle \\ &+\frac{V}{\sqrt{N}}\sum_{\mathbf{k}} e^{i\mathbf{k}\cdot\mathbf{R}_i}\langle\langle d^{\dagger}_{\mathbf{k},-\sigma}f_{i,\sigma}f_{i,-\sigma}, f^{\dagger}_{j,\sigma}\rangle\rangle \ .\end{aligned} \tag{3}$$

Here, we have three different new two-particle Green functions in Eq. (3), for each of which we set up the equation of motion again,

$$(\omega-\varepsilon_{\mathbf{k}})\langle\langle d_{\mathbf{k},\sigma}n_{i,-\sigma}, f^{\dagger}_{j,\sigma}\rangle\rangle=\frac{V}{\sqrt{N}}\sum_l e^{i\mathbf{k}\cdot\mathbf{R}_l}\langle\langle f_{l,\sigma}n_{i,-\sigma}, f^{\dagger}_{j,\sigma}\rangle\rangle \ , \tag{4}$$

$$\begin{aligned}(\omega-\varepsilon_{\mathbf{k}})\langle\langle d_{\mathbf{k},-\sigma}f^{\dagger}_{i,-\sigma}f_{i,\sigma}, f^{\dagger}_{j,\sigma}\rangle\rangle &= -\langle f^{\dagger}_{j,-\sigma}d_{\mathbf{k},-\sigma}\rangle\delta_{ij}-\frac{V}{\sqrt{N}}\sum_l e^{i\mathbf{k}\cdot\mathbf{R}_l}\langle\langle f^{\dagger}_{i,-\sigma}f_{l,-\sigma}f_{i,\sigma}, f_{j,\sigma}\rangle\rangle+\frac{V}{\sqrt{N}}\sum_{\mathbf{k}'} e^{i\mathbf{k}'\cdot\mathbf{R}_i}\langle d^{\dagger}_{\mathbf{k}',-\sigma}d_{\mathbf{k},-\sigma}\rangle\langle\langle f_{i,\sigma}, f^{\dagger}_{j,\sigma}\rangle\rangle \\ &-\frac{V}{\sqrt{N}}\sum_{\mathbf{k}'} e^{-i\mathbf{k}'\cdot\mathbf{R}_i}\langle f^{\dagger}_{i,-\sigma}d_{\mathbf{k},-\sigma}\rangle\langle\langle d_{\mathbf{k}',\sigma}, f^{\dagger}_{j,\sigma}\rangle\rangle \ ,\end{aligned} \tag{5}$$

$$\begin{aligned}(\omega+\varepsilon_{\mathbf{k}}-2\varepsilon_f-U)\langle\langle d^{\dagger}_{\mathbf{k},-\sigma}f_{i,\sigma}f_{i,-\sigma}, f^{\dagger}_{j,\sigma}\rangle\rangle &= -\langle d^{\dagger}_{\mathbf{k},-\sigma}f_{j,-\sigma}\rangle\delta_{ij}+\frac{V}{\sqrt{N}}\sum_l e^{-i\mathbf{k}\cdot\mathbf{R}_l}\langle\langle f^{\dagger}_{l,-\sigma}f_{i,-\sigma}f_{i,\sigma}, f^{\dagger}_{j,\sigma}\rangle\rangle-\frac{V}{\sqrt{N}}\sum_{\mathbf{k}'} e^{-i\mathbf{k}'\cdot\mathbf{R}_i}\langle d^{\dagger}_{\mathbf{k},-\sigma}f_{i,-\sigma}\rangle\langle\langle d_{\mathbf{k}',\sigma}, f^{\dagger}_{j,\sigma}\rangle\rangle \\ &-\frac{V}{\sqrt{N}}\sum_{\mathbf{k}'} e^{-i\mathbf{k}'\cdot\mathbf{R}_i}\langle d^{\dagger}_{\mathbf{k},-\sigma}d_{\mathbf{k}',-\sigma}\rangle\langle\langle f_{i,\sigma}, f^{\dagger}_{j,\sigma}\rangle\rangle \ .\end{aligned} \tag{6}$$

In Eqs. (5) and (6) decoupling approximations are made for the nondirectly correlating two-particle Green functions, which are represented as a product of the average and the one-particle Green function. Furthermore, the f-electron two-particle Green functions on the right-hand side of Eqs. (4)–(6) are decoupled only when site l is different from site i, in which case no one-site interaction U operates. For example, in Eq. (5) for $l\neq i$,

$$\langle\langle f^{\dagger}_{i,-\sigma}f_{l,-\sigma}f_{i,\sigma}, f^{\dagger}_{j,\sigma}\rangle\rangle$$

is reduced to

$$\langle f^{\dagger}_{i,-\sigma}f_{l,-\sigma}\rangle\langle\langle f_{i,\sigma}, f^{\dagger}_{j,\sigma}\rangle\rangle$$

but for $l=i$,

$$\langle\langle f^{\dagger}_{i,-\sigma}f_{l,-\sigma}f_{i,\sigma}, f^{\dagger}_{j,\sigma}\rangle\rangle$$

is treated without decoupling. Therefore, this Green-function decoupling approximation, which was made in the third stage of the hierarchy of the equations of motion, amounts to taking into account the on-site f-electron Coulomb correlation induced by hybridization V up to the order of $O(V^2)$. Apart from the different treatments of the on-site and off-site two-f-electron Green functions and the summations with the Bloch phase factor [$\exp(i\mathbf{k}\cdot\mathbf{R}_l)$, etc.] over sites and momenta $\mathbf{k}'$, this decoupling approximation is essentially the same as the Nagaoka decoupling in the impurity s-d model[24] and those of Theumann[22] and Lacroix[23] in the impurity Anderson model.

In order to obtain the f-electron Green function $\langle\langle f_{i,\sigma}, f^{\dagger}_{j,\sigma}\rangle\rangle$ one substitutes the two-particle Green functions appearing on the left-hand side of Eqs. (4)–(6) into Eq. (3) and that of Eq. (3) into Eq. (2), and one hopes to solve for $\langle\langle f_{i,\sigma}, f^{\dagger}_{j,\sigma}\rangle\rangle$ self-consistently. However, it is easier here to solve for the $\mathbf{k}$ representation $\langle\langle f_{\mathbf{k},\sigma}, f^{\dagger}_{\mathbf{k}',\sigma}\rangle\rangle$ instead of the site representation $\langle\langle f_{i,\sigma}, f^{\dagger}_{j,\sigma}\rangle\rangle$ through the Fourier transform of Eq. (2),

$$\left[\omega-\varepsilon_f-\frac{V^2}{\omega-\varepsilon_{\mathbf{k}}}\right]\langle\langle f_{\mathbf{k},\sigma}, f^{\dagger}_{\mathbf{k}',\sigma}\rangle\rangle = \delta_{\mathbf{k}\mathbf{k}'}+\frac{U}{N}\sum_{i,j} e^{i(\mathbf{k}\cdot\mathbf{R}_i-\mathbf{k}'\cdot\mathbf{R}_j)}\langle\langle f_{i,\sigma}n_{i,-\sigma}, f^{\dagger}_{j,\sigma}\rangle\rangle \ . \tag{7}$$

By representing the mixed Green functions such as $\langle\langle d_{\mathbf{k}',\sigma}, f^{\dagger}_{j,\sigma}\rangle\rangle$ in terms of the f-electron Green functions through their equations of motion one obtains the equation to determine $\langle\langle f_{\mathbf{k},\sigma}, f^{\dagger}_{\mathbf{k}',\sigma}\rangle\rangle$ after a little calculation,

$$\left[\omega-\varepsilon_f-B(\omega)-\frac{V^2}{\omega-\varepsilon_{\mathbf{k}}}A(\omega)\right]\langle\langle f_{\mathbf{k},\sigma},f^\dagger_{\mathbf{k}',\sigma}\rangle\rangle-\sum_{\mathbf{q}(\neq 0)}\left[D(\omega,-\mathbf{q})+\frac{V^2}{\omega-\varepsilon_{\mathbf{k}+\mathbf{q}}}C(\omega,\mathbf{q})\right]\langle\langle f_{\mathbf{k}+\mathbf{q},\sigma},f^\dagger_{\mathbf{k}',\sigma}\rangle\rangle$$
$$=\left[1+\frac{U\langle n_{i,-\sigma}\rangle}{\omega-\varepsilon_f-U+2i\Delta}\right]\delta_{\mathbf{k}\mathbf{k}'}+C(\omega,\mathbf{k}'-\mathbf{k}) , \tag{8}$$

where

$$A(\omega)=1+\frac{U\langle n_{i,-\sigma}\rangle}{\omega-\varepsilon_f-U+2i\Delta}+C(\omega,0) , \tag{9}$$

$$B(\omega)=D(\omega,0)-\frac{U\langle n_{i,-\sigma}\rangle}{\omega-\varepsilon_f-U+2i\Delta}\frac{V^2}{N}\sum_{\mathbf{k}_1}\left[\frac{2}{\omega-\varepsilon_{\mathbf{k}_1}}+\frac{1}{\omega+\varepsilon_{\mathbf{k}_1}-2\varepsilon_f-U}\right] , \tag{10}$$

$$C(\omega,\mathbf{q})=-\frac{U}{\omega-\varepsilon_f-U+2i\Delta}\frac{V}{N}\sum_{\mathbf{k}_1}\left[\frac{\langle f^\dagger_{\mathbf{k}_1+\mathbf{q},-\sigma}d_{\mathbf{k}_1,-\sigma}\rangle}{\omega-\varepsilon_{\mathbf{k}_1}}-\frac{\langle d^\dagger_{\mathbf{k}_1,-\sigma}f_{\mathbf{k}_1-\mathbf{q},-\sigma}\rangle}{\omega+\varepsilon_{\mathbf{k}}-2\varepsilon_f-U}\right] , \tag{11}$$

$$D(\omega,\mathbf{q})=-\frac{U}{\omega-\varepsilon_f-U+2i\Delta}\frac{V^2}{N}\sum_{\mathbf{k}}\left[(\langle d^\dagger_{\mathbf{k}_1+\mathbf{q},-\sigma}d_{\mathbf{k}_1,-\sigma}\rangle-\langle f^\dagger_{\mathbf{k}_1+\mathbf{q},-\sigma}f_{\mathbf{k}_1,-\sigma}\rangle)\frac{1}{\omega-\varepsilon_{\mathbf{k}_1}}\right.$$
$$\left.+(\langle d^\dagger_{\mathbf{k}_1,-\sigma}d_{\mathbf{k}_1-\mathbf{q},-\sigma}\rangle-\langle f^\dagger_{\mathbf{k}_1,-\sigma}f_{\mathbf{k}_1-\mathbf{q},-\sigma}\rangle)\frac{1}{\omega+\varepsilon_{\mathbf{k}_1}-2\varepsilon_f-U}\right] , \tag{12}$$

and $\Delta\equiv\pi\rho V^2$ with the constant density $\rho=1/2D$ of conduction-band states ($2D$ denoting the bandwidth).

On the other hand, the conduction-electron Green function $\langle\langle d_{\mathbf{k},\sigma},d^\dagger_{\mathbf{k}',\sigma}\rangle\rangle$ can be represented in terms of the f-electron Green function from the equations of motion as

$$\langle\langle d_{\mathbf{k},\sigma},d^\dagger_{\mathbf{k}',\sigma}\rangle\rangle=\frac{\delta_{\mathbf{k}\mathbf{k}'}}{\omega-\varepsilon_{\mathbf{k}}}+\frac{V^2}{(\omega-\varepsilon_{\mathbf{k}})(\omega-\varepsilon_{\mathbf{k}'})}\langle\langle f_{\mathbf{k},\sigma},f^\dagger_{\mathbf{k}',\sigma}\rangle\rangle . \tag{13}$$

Hereafter, we discuss the case of the infinite Coulomb repulsion $U=\infty$ which is the simplest assumption often made to represent the situations of the Kondo lattice and valence-fluctuation systems. In this large U limit the expressions (9)–(12) become

$$A(\omega)=1-\langle n_{i,-\sigma}\rangle+C(\omega,0) , \tag{14}$$

$$B(\omega)=D(\omega,0)+\frac{V^2}{N}\sum_{\mathbf{k}_1}\frac{2\langle n_{i,-\sigma}\rangle}{\omega-\varepsilon_{\mathbf{k}_1}} , \tag{15}$$

$$C(\omega,\mathbf{q})=-\frac{V}{N}\sum_{\mathbf{k}_1}\frac{\langle f^\dagger_{\mathbf{k}_1+\mathbf{q},-\sigma}d_{\mathbf{k}_1,-\sigma}\rangle}{\omega-\varepsilon_{\mathbf{k}_1}} , \tag{16}$$

$$D(\omega,\mathbf{q})=\frac{V^2}{N}\sum_{\mathbf{k}_1}\frac{\langle d^\dagger_{\mathbf{k}_1+\mathbf{q},-\sigma}d_{\mathbf{k}_1,-\sigma}\rangle-\langle f^\dagger_{\mathbf{k}_1+\mathbf{q},-\sigma}f_{\mathbf{k}_1,-\sigma}\rangle}{\omega-\varepsilon_{\mathbf{k}_1}} . \tag{17}$$

B. The Green functions and the self-consistent integral equation

So far we have retained in Eq. (8) the off-diagonal terms which have the off-diagonal momentum averages of various electron occupancies such as

$$\langle d^\dagger_{\mathbf{k}_1-\mathbf{q},-\sigma}d_{\mathbf{k}_1,-\sigma}\rangle ,$$

etc. In the case of the lattice the off-diagonal averages are in general of order $O(1/N)$ smaller than the diagonal ones, except in an impurity phenomenon. So, if the off-diagonal Green functions $\langle\langle f_{\mathbf{k}+\mathbf{q},\sigma},f^\dagger_{\mathbf{k},\sigma}\rangle\rangle$ ($\mathbf{q}\neq 0$) in the second term on the left-hand side (lhs) of Eq. (8) (for $\mathbf{k}'=\mathbf{k}$) are represented by the diagonal ones and substituted back into it, then it is seen that these terms are negligible. This is because a single off-diagonal factor has become a product of two off-diagonal factors of the average and the Green function by the decoupling treatment. Therefore, the decoupling scheme we use is equivalent to neglecting these off-diagonal terms, and one must go to a higher-stage decoupling approximation in order to take into account the $\mathbf{k}$ dependence of the self-energy. However, the lattice self-energy which results from the present treatment is qualitatively different from the single-site self-energy of the impurity system which is often used as an approximation for the lattice system.[17,32,33] As we shall see later, in the Kondo effects of the impurity system these off-diagonal terms become of the same order as the diagonal terms and play important roles characteristic of impurity in the behaviors of the self-energy and the Green functions.

Thus, one obtains the f-electron Green function from Eq. (8) as

$$\langle\langle f_{\mathbf{k},\sigma},f^\dagger_{\mathbf{k},\sigma}\rangle\rangle=\frac{A(\omega)}{\omega-\varepsilon_f-B(\omega)-\frac{V^2}{\omega-\varepsilon_{\mathbf{k}}}A(\omega)}=\frac{1}{R(\omega)^{-1}-\frac{V^2}{\omega-\varepsilon_{\mathbf{k}}}} , \tag{18}$$

with

$$R(\omega)=\frac{A(\omega)}{\omega-\varepsilon_f-B(\omega)} . \tag{19}$$

Using this expression (18) in Eq. (13) the conduction-electron Green function is written as

$$\langle\langle d_{\mathbf{k},\sigma},d^{\dagger}_{\mathbf{k},\sigma}\rangle\rangle=\frac{1}{\omega-\varepsilon_{\mathbf{k}}-V^2R(\omega)} . \tag{20}$$

These Green functions Eqs. (18) and (20) are essentially the same as those derived by Fedro and Sinha,[26] Costi,[27] and Baumgärtel and Müller-Hartmann[28] for the Anderson-lattice model, and the lattice extension of the impurity Green function obtained by Lacroix[23] and Theumann.[22] However, the detailed properties of these Green functions have not been so much studied numerically because of the difficulties in solving the self-consistent integral equation.[25] This is particularly true for the case of the Kondo limit that accompanies a sharp Kondo-resonance peak in the f-electron density of states. We investigate the characteristic features of the lattice Green functions in comparison with those of the impurity one by numerical calculations of the f-electron densities of states in both the Kondo regime and the valence-fluctuations regime. We are particularly interested in the difference between the impurity and the lattice Kondo effects.

Let us reduce the Green functions, Eqs. (18) and (20), i.e., the function $R(\omega)$, Eq. (19), to the self-consistent integral equation. We notice that $A(\omega)$ and $B(\omega)$ in $R(\omega)$ are related to the averages $\langle f^{\dagger}_{\mathbf{k},-\sigma}d_{\mathbf{k},-\sigma}\rangle$, $\langle d^{\dagger}_{\mathbf{k},-\sigma}d_{\mathbf{k},-\sigma}\rangle$, and $\langle f^{\dagger}_{\mathbf{k},-\sigma}f_{\mathbf{k},-\sigma}\rangle$ through $C(\omega,0)$ and $D(\omega,0)$. These average $\mathbf{k}$ dependent occupancies in turn can be represented using the imaginary parts of the Green functions. Here, we make the following approximations for the evaluations of the average occupancies: The $\mathbf{k}$ dependence of $\langle f^{\dagger}_{\mathbf{k},-\sigma}d_{\mathbf{k},-\sigma}\rangle$ and $\langle d^{\dagger}_{\mathbf{k},-\sigma}d_{\mathbf{k},-\sigma}\rangle$ is assumed to come only through that of the conduction-electron Green function, and the $\mathbf{k}$ dependence of $\langle f^{\dagger}_{\mathbf{k},-\sigma}f_{\mathbf{k},-\sigma}\rangle$ is that of the f-electron Green function. Thus, $C(\omega,0)$ and $D(\omega,0)$ can be expressed as follows:

$$C(\omega,0)=\frac{\rho V^2}{\pi}\int d\omega' f(\omega')\int\frac{d\varepsilon_{\mathbf{k}_1}}{\omega-\varepsilon_{\mathbf{k}_1}}\mathrm{Im}\frac{R(\omega')}{\omega'-\varepsilon_{\mathbf{k}_1}} , \tag{21}$$

$$D(\omega,0)=-F(\omega)-\frac{\rho V^2}{\pi}\int d\omega' f(\omega')\frac{d\varepsilon_{\mathbf{k}_1}}{\omega-\varepsilon_{\mathbf{k}_1}}\mathrm{Im}\frac{V^2R(\omega')}{(\omega'-\varepsilon_{\mathbf{k}_1})^2}$$
$$+\frac{\rho V^2}{\pi}\int d\omega' f(\omega')\int\frac{d\varepsilon_{\mathbf{k}_1}}{\omega-\varepsilon_{\mathbf{k}_1}}\mathrm{Im}\frac{1}{R(\omega')^{-1}-\dfrac{V^2}{\omega'-\varepsilon_{\mathbf{k}_1}}} , \tag{22}$$

where

$$\langle\langle d_{\mathbf{k}_1,-\sigma},f^{\dagger}_{\mathbf{k}_1,-\sigma}\rangle\rangle=V\langle\langle f_{\mathbf{k}_1,-\sigma},f^{\dagger}_{\mathbf{k}_1,-\sigma}\rangle\rangle/(\omega'-\varepsilon_{\mathbf{k}_1})$$

and Eq. (13) have been used in Eq. (21) and in the first two terms of Eq. (22), respectively, with the replacement of

$$\langle\langle f_{\mathbf{k}_1,-\sigma},f^{\dagger}_{\mathbf{k}_1,-\sigma}\rangle\rangle$$

by $R(\omega')$, and in the last term of Eq. (22) the expression (18) has been inserted for

$$\langle\langle f_{\mathbf{k}_1,-\sigma},f^{\dagger}_{\mathbf{k}_1,-\sigma}\rangle\rangle .$$

$f(\omega)$ is the Fermi distribution function and $F(\omega)$ is the Fermi-function integral given by

$$F(\omega)=\frac{\Delta}{\pi}\int_{-D}^{D}\frac{f(\omega')}{\omega'-\omega-i\eta}d\omega'$$
$$=\frac{\Delta}{\pi}\left[i\pi f(\omega)+\ln\frac{2\pi}{\beta D}+\mathrm{Re}\Psi\left[\tfrac{1}{2}-i\beta\frac{\omega-\epsilon_F}{2\pi}\right]\right] , \tag{23}$$

and $\eta=+0$, $\beta=1/T(k_B=1)$, and $\Psi(z)$ is the digamma function. In the expressions (21) and (22) the integrals over $\varepsilon_{\mathbf{k}_1}$ can be performed and one obtains

$$C(\omega,0)=\frac{\Delta}{\pi}\int\frac{R^*(\omega')f(\omega')}{\omega'-\omega-i\eta}d\omega' , \tag{24}$$

$$D(\omega,0)=-F(\omega)-i\frac{\Delta}{\pi}\int[\mathrm{Im}R(\omega')]f(\omega')d\omega'$$
$$+V^2\frac{\Delta}{\pi}\int\frac{[R^*(\omega')]^2f(\omega')}{\omega'-\omega-V^2R^*(\omega')}d\omega' , \tag{25}$$

where the last two terms in Eq. (25) come from $\langle f^{\dagger}_{\mathbf{k}_1,-\sigma}f_{\mathbf{k}_1,-\sigma}\rangle$ terms in Eq. (17). Therefore, Eqs. (19), (14)–(17), and (23)–(25) constitute the self-consistent integral equation to solve for $R(\omega)$,

$$R(\omega)=\frac{1-\langle n_{i,-\sigma}\rangle+C(\omega,0)}{\omega-\varepsilon_f^*+2i\Delta\langle n_{i,-\sigma}\rangle-D(\omega,0)} , \tag{26}$$

where

$$\varepsilon_f^*=\varepsilon_f+\frac{\Delta}{\pi}\langle n_{i,-\sigma}\rangle\ln\left[\frac{D+\omega}{D-\omega}\right] . \tag{27}$$

Then, once $R(\omega)$ is solved, the f-electron Green function $\langle\langle f_{\mathbf{k},\sigma},f^{\dagger}_{\mathbf{k},\sigma}\rangle\rangle$ can be calculated from Eq. (18). On

the other hand, the Green function in site representation for the periodic nonmagnetic states is written as

$$\langle\langle f_{i,\sigma} f_{i,\sigma}^{\dagger} \rangle\rangle = \frac{1}{N} \sum_{\mathbf{k}} \frac{1}{R(\omega)^{-1} - \dfrac{V^2}{\omega - \varepsilon_{\mathbf{k}}}} . \tag{28}$$

C. The single-impurity system and the single-site approximation of the lattice in the decoupling scheme

In this subsection we compare the lattice f-electron Green function obtained in Sec. II B with those of the single-impurity system and of the single-site approximation for the lattice system within the same decoupling scheme. The impurity f-electron Green function $\langle\langle f_{\sigma}, f_{\sigma}^{\dagger} \rangle\rangle_{\text{imp}}$ has been obtained by Lacroix[23] essentially in the same decoupling approximation, but it can be derived easily here from Eq. (8). Reducing the f-electron sites to the single site at the origin $\mathbf{R}_i = 0$, using the relationship

$$\langle\langle f_{\mathbf{k},\sigma}, f_{\mathbf{k}',\sigma}^{\dagger} \rangle\rangle = \frac{1}{N} \langle\langle f_{\sigma}, f_{\sigma}^{\dagger} \rangle\rangle_{\text{imp}} , \tag{29}$$

together with $f_{\sigma}^{\dagger} = (1/\sqrt{N}) \sum_{\mathbf{k}} f_{\mathbf{k}}^{\dagger}$ in Eq. (8), and then operating the summation $\sum_{\mathbf{k}}$ on both sides of Eq. (8) including the off-diagonal terms lead, for $U = \infty$, to the impurity Green function

$$\langle\langle f_{\sigma}, f_{\sigma}^{\dagger} \rangle\rangle_{\text{imp}} = \frac{A_{\text{imp}}(\omega)}{\omega - \varepsilon_f - B_{\text{imp}}(\omega) - \dfrac{V^2}{N} \sum_{\mathbf{k}} \dfrac{1}{\omega - \varepsilon_{\mathbf{k}}} A_{\text{imp}}(\omega)} \equiv \frac{1}{\omega - \varepsilon_f - \Sigma_{\text{imp}}(\omega) - \dfrac{V^2}{N} \sum_{\mathbf{k}} \dfrac{1}{\omega - \varepsilon_{\mathbf{k}}}} , \tag{30}$$

where

$$A_{\text{imp}}(\omega) = 1 - \langle n_{-\sigma} \rangle - \frac{V}{\sqrt{N}} \sum_{k_1} \frac{\langle f_{-\sigma}^{\dagger} d_{\mathbf{k}_1,-\sigma} \rangle}{\omega - \varepsilon_{\mathbf{k}_1}} , \tag{31}$$

$$B_{\text{imp}}(\omega) = \frac{V^2}{N} \sum_{\mathbf{k}_1,\mathbf{k}_2} \frac{\langle d_{\mathbf{k}_2,-\sigma}^{\dagger} d_{\mathbf{k}_1,-\sigma} \rangle + \langle n_{-\sigma} \rangle \delta_{\mathbf{k}_1\mathbf{k}_2}}{\omega - \varepsilon_{\mathbf{k}_1}} , \tag{32}$$

and Eq. (30) defines the impurity self-energy $\Sigma_{\text{imp}}(\omega)$.

Next, we derive the lattice f-electron Green function in the single-site approximation.[17,32,33] In this approximation the f-electron self-energy part due to Coulomb interaction U is treated on each site as an independent-site effect. The self-energy is therefore the same as that of the impurity Green function, Eq. (30), and is incoherent, contrary to the coherent treatment for the lattice Green function (and the self-energy), Eqs. (18) and (26), in Secs. II A and II B. The f-electron Green function itself in the single-site approximation, however, is treated as that of a coherent Bloch electron, as in Sec. II A and B. Now, one can derive the single-site Green function from the impurity self-energy $\Sigma_{\text{imp}}(\omega)$, but in order to elucidate the relationship between this approximation and that of the coherent treatment, we derive it from the equations of motion given earlier in Sec. II A. In the equations of motion Eqs. (3)–(6) we reduce those Bloch factors with the same wave numbers as those of the average quantities to unity, regarding that the scattered waves other than the propagators are confined to the single site $\mathbf{R}_i = 0$. Then, the similar calculations as before lead to the single-site Green function using the impurity functions $A_{\text{imp}}(\omega)$ and $B_{\text{imp}}(\omega)$ [Eqs. (31) and (32)] with the replacement of $\langle n_{-\sigma} \rangle$ by $\langle n_{i,-\sigma} \rangle$,

$$\begin{aligned} \langle\langle f_{\mathbf{k},\sigma}, f_{\mathbf{k},\sigma}^{\dagger} \rangle\rangle_s &= \frac{A_{\text{imp}}(\omega)}{\omega - \varepsilon_f - B_{\text{imp}}(\omega) - \dfrac{V^2}{\omega - \varepsilon_{\mathbf{k}}} A_{\text{imp}}(\omega)} \\ &= \frac{1}{G_{\text{imp}}(\omega)^{-1} + \dfrac{V^2}{N} \sum_{\mathbf{k}'} \dfrac{1}{\omega - \varepsilon_{\mathbf{k}'}} - \dfrac{V^2}{\omega - \varepsilon_{\mathbf{k}}}} \\ &= \frac{1}{\omega - \epsilon_f - \Sigma_{\text{imp}}(\omega) - \dfrac{V^2}{\omega - \varepsilon_{\mathbf{k}}}} , \end{aligned} \tag{33}$$

where

$$G_{\text{imp}}(\omega) \equiv \langle\langle f_{\sigma}, f_{\sigma}^{\dagger} \rangle\rangle_{\text{imp}}$$

and its expression (30) has been used together with the impurity self-energy $\Sigma_{\text{imp}}(\omega)$. The impurity self-energy $\Sigma_{\text{imp}}(\omega)$ defined in Eq. (30) is written as

$$\Sigma_{\text{imp}}(\omega) = \frac{1}{A_{\text{imp}}(\omega)} [B_{\text{imp}}(\omega) + (A_{\text{imp}}(\omega) - 1)(\omega - \varepsilon_f)] . \tag{34}$$

Therefore, the distinction between the two Green functions Eqs. (18) and (33) is whether or not the $\mathbf{k}$-dependent average quantities are treated as the coherent ones in the self-energy. The Green function in the site representation is written as

$$\langle\langle f_{i,\sigma}, f_{i,\sigma}^{\dagger} \rangle\rangle_s = \frac{1}{N} \sum_{\mathbf{k}} \frac{1}{G_{\text{imp}}(\omega)^{-1} + \dfrac{V^2}{N} \sum_{\mathbf{k}'} \dfrac{1}{\omega - \varepsilon_{\mathbf{k}'}} - \dfrac{V^2}{\omega - \varepsilon_{\mathbf{k}}}} . \tag{35}$$

That impurity Green function Eq. (30) is of course identical with that derived by Lacroix,[23] and the single-site Green function Eq. (35) has the same form as the f-electron Green function obtained by Grewe[17] in a perturbative method, where the self-energy is expanded by the skeleton diagrams essentially in the single-site approximation. So, within the same decoupling approximation the single-site Green functions used by Grewe and others[32,33] as well as the impurity Green function of Lacroix[23] can be examined with respect to the lattice Green function Eq. (18) in the present coherent treatment.

As in the lattice Green function in Sec. II B, the impurity Green function $G_{\rm imp}(\omega)$ in Eq. (30) also constitutes an integral equation similar to Eq. (26), because the average quantities in $A_{\rm imp}(\omega)$ and $B_{\rm imp}(\omega)$ must be determined using $G_{\rm imp}(\omega)$ in a self-consistent manner. Expressing these averages in terms of the imaginary parts of the Green functions and performing integrals over $\varepsilon_{\mathbf{k}_1}$ the following integral equation for $G_{\rm imp}(\omega)$ is obtained:[23]

$$G_{\rm imp}(\omega)=\frac{1-\langle n_{-\sigma}\rangle+\frac{\Delta}{\pi}\int\frac{G_{\rm imp}(\omega')^* f(\omega')}{\omega'-\omega-i\eta}d\omega'}{\omega-\varepsilon_f^*+i\Delta+F(\omega)+2\Delta i\frac{\Delta}{\pi}\int\frac{G_{\rm imp}(\omega')^* f(\omega')}{\omega'-\omega-i\eta}d\omega'}\ , \tag{36}$$

where Eq. (23) has been used, and here

$$\varepsilon_f^*=\varepsilon_f+\frac{\Delta}{\pi}\ln\left|\frac{D+\omega}{D-\omega}\right|\ . \tag{37}$$

The single-site Green function $\langle\langle f_{\mathbf{k},\sigma}, f^\dagger_{\mathbf{k},\sigma}\rangle\rangle_s$, Eq. (33), can be evaluated once the self-consistent solution of the impurity Green function is obtained.

Let us now compare the lattice f-electron Green functions in the coherent treatment, Eqs. (18), (26), and (28), with those of the impurity system, Eqs. (30) and (36), and of the single-site approximation of the lattice system, Eqs. (33) and (35). Apart from the presence of the coherent hybridization term reflecting the periodic system in the denominator of the lattice Green function $\langle\langle f_{\mathbf{k},\sigma}, f^\dagger_{\mathbf{k},\sigma}\rangle\rangle$, Eq. (18), it is the $R(\omega)$ function and its integral equation Eq. (26) that should be compared to the impurity Green function Eq. (36). Although $R(\omega)$ and $G_{\rm imp}(\omega)$ have similar forms, the important difference is the absence, in the denominator of the former $R(\omega)$, of the integral term with the infinitesimal imaginary denominator other than the common term $F(\omega)$, because this term can become dominant together with $F(\omega)$ at low temperature near $\omega\sim\epsilon_F$. This term comes from the incoherent treatment of the multiple scatterings due to Coulomb interaction at each site, and therefore also exists in the single-site Green function $\langle\langle f_{\mathbf{k},\sigma}, f^\dagger_{\mathbf{k},\sigma}\rangle\rangle_s$, Eq. (33). Actually, it originates both from the off-diagonal $\langle d^\dagger_{\mathbf{k}_2,-\sigma} d_{\mathbf{k}_1,-\sigma}\rangle$ terms of $B_{\rm imp}(\omega)$, Eq. (32), and the last term of $A_{\rm imp}(\omega)$, Eq. (31). These terms from independent-site incoherent Coulomb scatterings are valid and should be present in the impurity system, but are not justified in the periodic system, especially when they become dominant. It is not clear whether Grewe's impurity Green function $G_{\rm imp}(\omega)$ actually contains these terms or not. Other differences between $R(\omega)$ and $G_{\rm imp}(\omega)$ are minor and details; e.g., while the broadening $i\Delta$ and/or the f-level shift $\Delta\varepsilon_f=\varepsilon_f^*-\varepsilon_f$ come from the one-body hybridization in the impurity and the single-site systems, they ($2i\Delta\langle n_{i,-\sigma}\rangle$, etc., and $\Delta\varepsilon_f$) arise from the Coulomb interaction plus hybridization in $R(\omega)$ and would vanish for $U=0$. [There are of course the broadening and the shift from $F(\omega)$ in both cases.] Finally, we point out that the absence of the incoherent integral term in the denominator of the $R(\omega)$ function in the lattice case leads to the small imaginary parts of f-electron self-energy at low temperatures over a finite range of ω around the Fermi energy.

III. CHARACTERISTIC TEMPERATURES

In this section we explore the characteristic temperatures of the impurity and lattice systems in the Kondo limit from the Green functions obtained in Sec. II. We find that in the single-impurity Anderson model there is only one characteristic temperature T_K for the Kondo resonance, whereas in the Anderson-lattice model there exist two characteristic temperatures of several times T_K and T_0, respectively, for the onset and completion of the crossover from the incoherent Kondo-resonance to the coherent Kondo-lattice (heavy-fermion) state. In the latter, however, T_0 can be expressed in terms of T_K which becomes the only temperature scale.

A. The single-impurity Anderson model

The Kondo temperature T_K is often defined as the characteristic temperature to give rise to the Kondo resonance at the Fermi energy in the f-electron density of states.[23,25,26,1,35] We give here the Kondo-resonance temperature T_K for the single-impurity model including the orbital-degenerate case.

At low temperature and for $\omega'\sim\epsilon_F$ the ω' dependence of $G_{\rm imp}(\omega')^*$ in Eq. (36) can be shown to have a slow logarithmic behavior across ϵ_F as compared to the other integrand functions in the integrals. Thus, just for the purpose of discussing the characteristic temperatures, $G_{\rm imp}(\omega')^*$ in the integrand can be represented by the value $G_{\rm imp}(\omega)^*$ for $\omega'=\omega$, and the self-consistent integral equation (36) can be approximated by the algebraic one, ($\varepsilon_f^*=\varepsilon_f$),

$$G_{\rm imp}(\omega)=\frac{1-\langle n_{-\sigma}\rangle+G_{\rm imp}(\omega)^* F(\omega)}{\omega-\varepsilon_f+i\Delta+F(\omega)+2i\Delta G_{\rm imp}(\omega)^* F(\omega)}\ , \tag{38}$$

as was done by Lacroix.[23] We have checked this approximation numerically in detail and confirmed its accuracy. To solve this self-consistent equation one puts $G_{\rm imp}(\omega)=x(\omega)+iy(\omega)$, whose imaginary part $y(\omega)$ gives the f-electron density of states by

$$\rho_f^{\rm imp}(\omega)=(-1/\pi)\,{\rm Im}G_{\rm imp}(\omega)=-y(\omega)/\pi\ .$$

From Eq. (38) $y(\omega)$ is calculated in the approximation $\Delta/(\epsilon_F-\varepsilon_f)\ll 1$ and is obtained as

$$y(\omega)=\frac{1}{2}\left\{-\frac{\varepsilon+2\alpha}{2\alpha\Delta}-\left[\left[\frac{\varepsilon+2\alpha}{2\alpha\Delta}\right]^2-\frac{4p}{\varepsilon}\left[\frac{p}{\varepsilon}+\frac{1}{2\alpha}\right]\right]^{1/2}\right\}, \tag{39}$$

where

$$\varepsilon=\omega-\varepsilon_f\ , \tag{40}$$

$$\alpha=F(\omega)-i\Delta f(\omega)\ , \tag{41}$$

and

$$p=1-\langle n_{-\sigma}\rangle\ . \tag{42}$$

An examination of the expression (39) for $y(\omega)$ yields the following characteristic f-electron densities of states near the Kondo-resonance peak at the respective energies ω for $T=0$ or for the temperatures T at $\omega=\epsilon_F$. While the Kondo-resonance peak $\rho_f^{\rm imp}(\omega)\sim 1/\pi\Delta$ is realized at $\omega\sim\epsilon_F$ (approximately at ϵ_F because of the approximate treatment above) for $T=0$, the half-peak $\rho_f^{\rm imp}(\omega)\sim 1/2\pi\Delta$ is obtained at the Kondo energy $|\omega-\epsilon_F|=T_K$ for $T=0$ or at $\omega=\epsilon_F$ for the Kondo temperature $T=T_K$. On the other hand, while for $|\omega-\epsilon_F|\gg T_K$ at $T=0$ or for $T\gg T_K$ at $\omega=\epsilon_F$,

$$\rho_f^{\rm imp}(\omega)\sim(1/2\pi)\Delta/(\omega-\varepsilon_f)^2$$

is obtained as the tail of the f-level resonance peak at ε_f^*, the energy $|\omega-\epsilon_F|=T_K'$ at $T=0$ and the temperature $T=T_K'$ at $\omega=\epsilon_F$ give the increase of the Kondo-resonance peak by $\rho_f^{\rm imp}(\omega)\sim 1/\pi(\epsilon_F-\varepsilon_f)$. These two temperatures T_K and T_k' are obtained from Eq. (39) as follows:

$$T_K=1.14\ {\rm D}\exp\left[\frac{\pi(\epsilon_F-\varepsilon_f)}{\Delta}\right], \tag{43}$$

$$T_K'=1.14\ {\rm D}\exp\left[\frac{\pi(\epsilon_F-\varepsilon_f)}{2\Delta}\right]. \tag{44}$$

Therefore, in the present nondegenerate impurity model the Kondo resonance appears very close to the Fermi energy ϵ_F and the height and the width of the resonance peak at $T=0$ are $\sim 1/\pi\Delta$ and $\sim T_K$, respectively.

These results carry on to the N_f-orbital-degenerate Anderson model with the spin-orbit coupling in the present treatment but is in sharp contrast with the results[3,25,35] obtained in the large orbital-degeneracy limit, $N_f\to\infty$, $V^2\to 0$ with $N_fV^2=$constant, as is shown below. Similar discussions can be made for the Kondo resonance if one makes the following model assumption which is unrealistic but commonly used[25,35,36] to deal with the orbital-degenerate models; the component M of the total angular-momentum quantum number j of an f electron in the spin-orbit level with degeneracy $N_f=2j+1$ is conserved in the hybridization mixing with a band electron. The f-electron Green function[25] for each channel M can thus be obtained and approximated for $\omega\sim\epsilon_F$ at low temperatures as

$$G_{\rm imp}(\omega)=\frac{\langle n_f\rangle/N_f+G_{\rm imp}(\omega)^*(N_f-1)F(\omega)}{\omega-\varepsilon_f+i\Delta+(N_f-1)F(\omega)+2i\Delta G_{\rm imp}(\omega)^*(N_f-1)F(\omega)}\ . \tag{45}$$

By solving this equation as before, one finds that the position of the Kondo resonance for $T=0$ lies very close to ϵ_F with the peak height $\sim 1/\pi\Delta$ and the width $\sim T_K$, which is, in this case, given by

$$T_K=1.14\ {\rm D}\exp\left[-\frac{\pi(\epsilon_F-\varepsilon_f)}{(N_f-1)\Delta}\right]. \tag{46}$$

On the other hand, in the large orbital-degeneracy limit[25,35] the last term in the Green function denominator in Eq. (45) can be neglected,[25] and the position of the Kondo-resonance peak comes to $\omega\sim T_K$ [Eq. (46)] with the height $\sim 1/\pi\tilde{\Delta}$ [$\tilde{\Delta}\equiv(N_f-1)\Delta$] and the width $\sim T_K$ for the total of all the N_f channels.[27,35,3]

B. The Anderson-lattice model

The f-electron density of states is defined by

$$\rho_f(\omega)=-\frac{1}{\pi}\frac{1}{N}\sum_{\mathbf{k}}{\rm Im}\langle\langle f_{\mathbf{k},\sigma},f_{\mathbf{k},\sigma}^\dagger\rangle\rangle\ , \tag{47}$$

and is expressed in terms of the function $R(\omega)$ of Eq. (26) using Eq. (18) and carrying out the summation over $\mathbf{k}$,

$$\rho_f(\omega)=-\frac{1}{\pi}\,{\rm Im}\left\{R(\omega)\left[1-\frac{\Delta}{\pi}R(\omega){\rm Ln}\left[\frac{D-\omega+V^2R(\omega)}{-D-\omega+V^2R(\omega)}\right]\right]\right\}. \tag{48}$$

(Here, $\mathrm{Ln}z = \ln|z| + i\arg z$, $-\pi < \arg z \leq \pi$.) Since Δ is small (typically $\Delta/D \ll 1$) for the relevant systems, the second term in $\rho_f(\omega)$ is negligible unless $R(\omega)$ becomes of order $O(\Delta^{-1})$, and the f-electron density of states $\rho_f(\omega)$ is usually determined by $R(\omega)$ at high temperatures. As temperature is decreased, the function $R(\omega)$ grows and the density of states $\rho_f(\omega)$ starts to form a broad resonance near the Fermi energy, but the second term in Eq. (48) does not become large enough to contribute down to a temperature of several times T_K [Eq. (43)]. Therefore, this is the so-called incoherent Kondo resonance that takes place at individual sites of the Kondo-lattice system before the second-term contribution of $\rho_f(\omega)$ from the **k**-dependent origin sets in, i.e., the **k**-independent resonance in $R(\omega)$ corresponding to the impurity Kondo resonance in $G_{\mathrm{imp}}(\omega)$. As temperature is further decreased below several times T_K, the Kondo resonance starts to split due to the second term, which signals the onset of the effect of the **k**-dependence, i.e., that of the crossover to the coherent Kondo-lattice state. Contrary to the picture that in the Kondo-lattice state the coherence sets in after the individual-site Kondo effects are fully accomplished, the crossover to the coherent Kondo state starts at a temperature above T_K and thus the lattice Kondo effect is distinguished from the impurity Kondo effect.

In the crossover transition from the incoherent to the coherent Kondo state, at first the coherent lower-energy peak is produced at ϵ_F, and the higher-energy one at an energy ω, approximately equal to several $T_K - 10T_K$ above ϵ_F, with the dip between the split peaks being located at ω approximately equal to the temperature T above ϵ_F. With a decrease in temperature, the coherent lower-energy peak becomes higher and sharper with the position being shifted slightly of order $O(T_K)$ below ϵ_F, and the dip becomes deeper and sharper with the position ω_d approaching ϵ_F with the relationship $\omega_d \sim T$, whereas the higher-energy peak remains as a broad peak at the same position. Here, there seems to exist a characteristic temperature for the coherent Kondo-lattice state. Below the temperature $\sim 0.1T_K$, the height and position of the sharp coherent peak and the entire spectrum around ϵ_F stay the same, except the dip which further tends to become a deeper pseudogap on the Fermi energy ϵ_F as temperature is reduced. We assume that at this temperature $\sim 0.1T_K$, the coherence is fully developed between the individual Kondo sites, and we call it the coherence temperature T_0. Therefore, below T_0 ($\sim 0.1T_K$) the Kondo lattice is essentially the coherent Kondo state, and its complete coherence is further achieved by reducing the small imaginary part of the self-energy at lower temperatures. The sharp coherent lower-energy f-electron peak is responsible for producing the heavy quasiparticle fermions. The stable heavy-fermion quasiparticle band is formed below T_0 but decays quickly with temperature above T_0 because the sharp coherent lower-energy peak decays above it. Therefore, it is not the heavy-fermion quasiparticle bandwidth [$\sim O(T_K)$] but its stability temperature (binding energy) that determines the coherence temperature T_0 and the low-temperature properties. In the crossover temperature range $T_0 < T <$ several T_K there arises the problem of disorder for impuritylike Kondo resonances at individual sites.

IV. f-ELECTRON DENSITY OF STATES

The densities of states of f electrons $\rho_f(\omega)$ are calculated numerically as functions of temperature for the infinite Coulomb repulsion $U = \infty$ in the valence-fluctuation regime, as well as in the Kondo-lattice regime of the Anderson lattice model. In order to study the structures of the coherent heavy-fermion peak, the incoherent Kondo-resonance peak, and the valence-fluctuation peaks in the f-electron densities of states near ϵ_F, we have performed the following self-consistent calculations of $\rho_f(\omega)$ as accurately as possible.

First, for a constant f-electron number per site $n_f \equiv \langle n_f \rangle = 2\langle n_{i,-\sigma} \rangle$ the integral equation for the function $R(\omega)$, Eqs. (26) and (23)–(25), is solved until the self-consistency is attained within the accuracy of 2% for each ω. Then, the densities of states $\rho_f(\omega)$ are calculated by Eq. (48). Using the resultant densities of state $\rho_f(\omega)$ we have computed $\langle n_{i,-\sigma} \rangle$ which is compared with the previous $\langle n_{i,-\sigma} \rangle$. This set of calculations has been repeated until the f-electron number per site n_f becomes self-consistent within 1%. As a result, $\rho_f(\omega)$ has also become self-consistent within an accuracy of 2%. In order to compare the lattice Kondo resonance with the impurity Kondo resonance the impurity densities of states $\rho_f^{\mathrm{imp}}(\omega)$ are also calculated in the Kondo regime for the same parameters. The similar self-consistent calculations of the Green functions $G_{\mathrm{imp}}(\omega)$ corresponding to those of $R(\omega)$ are carried out by solving the integral equation Eq. (36) with the same accuracy. The total electron number n per site in the Kondo regime is not fixed for different temperatures, but as we will see, the f-electron number n_f as well as the total one n does not change below some temperatures (~ 200 K).

We show in Fig. 1 the f-electron densities of states $\rho_f^{\mathrm{imp}}(\omega)$ as functions of temperature for the impurity Anderson model in the Kondo regime with $T_K = 4.3$ K. As temperature decreases, it is seen that the Kondo resonance starts to appear[23] at $\omega \sim \epsilon_F$ near the onset temperature $T_K' = 224$ K and grows to half the full peak at the Kondo temperature $T_K = 4.3$ K. For $T \to 0$ the height, the position, and the width of this resonance peak agree approximately with the analytical results, $1/\pi\Delta \simeq 2$, $\omega \sim \epsilon_F$, and $\sim T_K$ ($= 4.3$ K), respectively. The Kondo resonance has a skew line shape around ϵ_F in this infinite U asymmetric Anderson model.

The f-electron densities of states $\rho_f(\omega)$ of the Anderson lattice model are shown in Fig. 2 for the same Kondo-regime parameters. It is noticed that with decrease in temperature, the f-electron spectra start to create the incoherent Kondo-resonance peak ($T = 200$ K) near the impurity onset temperature $T_K' = 224$ K. At a temperature of about several T_K ($T \sim 20$ K) the Kondo resonance begins to split into the lower-energy peak at $\omega \sim \epsilon_F$ and the higher-energy one

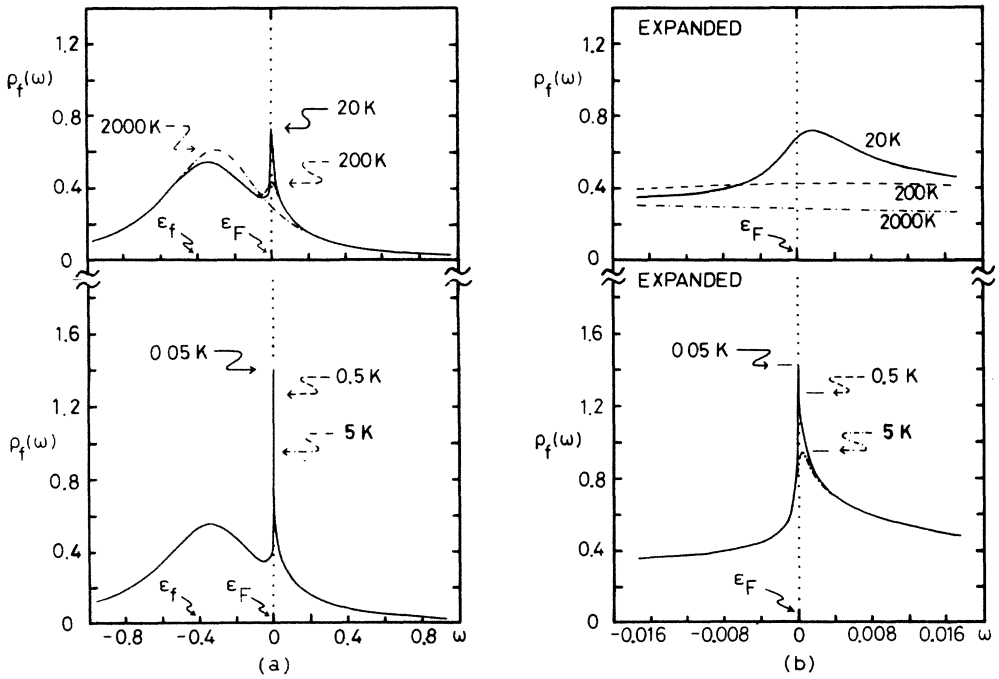

FIG. 1. Temperature-dependent f-electron density of states $\rho_f^{\text{imp}}(\omega)$ [(a) and (b)] for the single-impurity system in the Kondo regime. (b) is the expanded scale. The Kondo-resonance peak appears near ϵ_F for $T \sim T_K'$ (=224 K) [Eq. (44)], grows to $\sim 1/2\pi\Delta = 1$ for $T = T_K$ (=4.3 K) [Eq. (43)] and saturates at $1/\pi\Delta = 2$ for $T = 0$ K. Notice that the resonance peak comes very close to ϵ_F for $T < T_K$, and the half width is about T_K. $\varepsilon_f = -0.4$, $V = 0.32$, $U = \infty$, $\pi\Delta = 0.5$, $\epsilon_F = 0$, $\rho = \frac{1}{2}$, and $D = 1 (-D \leq \varepsilon_k \leq D)$. $n_f = 0.82$ for $T \leq 1000$ K.

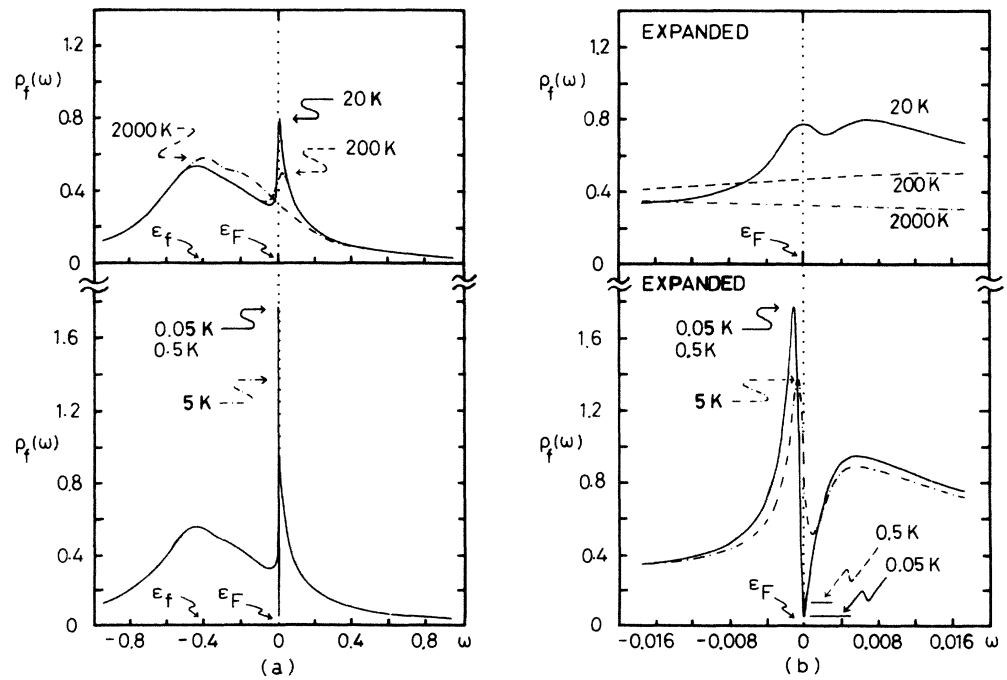

FIG. 2. Temperature-dependent f-electron density of states $\rho_f(\omega)$ [(a) and (b)] of the Anderson-lattice model in the Kondo regime for the same parameters as Fig. 1 [(b) is expanded scale]. The incoherent Kondo lattice resonance arises for $T \sim T_K'$ (=224 K) and splits, for $T \sim$ several T_K (=4.3 K), into the low-energy, sharp coherent peak, starting on ϵ_F and shifting to $\omega \sim T_K$ below ϵ_F, and the high-energy, broad incoherent peak at $\omega \sim 10T_K$. The dip at $\omega \sim T$ becomes a sharp pseudogap for $T < T_K$. The temperature dependences of the entire $\rho_f(\omega)$ structures stop at $T \sim 0.1T_K$ except the vanishing pseudogap on ϵ_F. $n_f = 0.73$ for $T \leq 1000$ K.

at $\omega \sim 10T_K$ ($T_K = 4.3$ K). As temperature is reduced, the former peak shifts slightly [of order $O(T_K)$] below ϵ_F, becomes sharper and grows, while the latter one remains almost the same. The dip between the two peaks becomes deeper and its position is always located at about $\omega \sim T$, approaching ϵ_F as $T \to 0$. As one can notice in Fig. 2, for temperatures below $T_0 \sim 0.1T_K$ the sharp lower-energy coherent peak and other $\rho_f(\omega)$ structures around ϵ_F except the narrow dip are stabilized and do not change. The height of the sharp peak below $T_0 \sim 0.1T_K$ is $\lesssim 1/\pi\Delta$ and the peak position is about T_K, but the width is a little wider (approximately several T_K) than the impurity Kondo-resonance peak. Here, the relative positions of the sharp peak and the dip with respect to ϵ_F are very accurate and reliable, being irrelevant of the uncertainty of the absolute Fermi-level position ϵ_F due to the resolution (1%) of the self-consistent total electron number, because these structures move together in precisely the same relative positions with the small shift of ϵ_F. As to the f-level resonance at ε_f^*, the periodic system, which would have two hybridization-split peaks under vanishing or small Coulomb repulsion U, has a single broad peak in the Kondo regime due to the many-body hybridization broadening effects under strong Coulomb interaction, as discussed at the end of Sec. II C, which is in agreement with the result obtained by perturbation expansion in U at $T=0$.[37]

The temperature dependence of the conduction-electron densities of states $\rho_c(\omega)$ per lattice site is also studied for the same Kondo-regime parameters as in Fig. 2. $\rho_c(\omega)$ is expressed in terms of the function $R(\omega)$ of Eq. (26) using Eq. (20) and carrying out the summation over $\mathbf{k}$,

$$\rho_c(\omega) = -\frac{1}{\pi}\frac{1}{N}\sum_{\mathbf{k}} \mathrm{Im}\langle\langle d_{\mathbf{k},\sigma}, d^{\dagger}_{\mathbf{k},\sigma}\rangle\rangle$$

$$= \frac{\rho}{\pi}\,\mathrm{Im}\left[\mathrm{Ln}\left[\frac{D-\omega+V^2R(\omega)}{-D-\omega+V^2R(\omega)}\right]\right], \qquad (49)$$

where Ln is understood as before and the noninteracting conduction density of states $\rho = 1/2D = 0.5$ is used. Figure 3 illustrates the temperature variations of the $\rho_c(\omega)$ curve with a sharp dip at $\omega \gtrsim \epsilon_F$ which corresponds to that of $\rho_f(\omega)$ but is much deeper than the latter. Again, the bottom of the dip is situated at $\omega \sim T$ and approaches ϵ_F as T tends to 0 K.

Figure 4 shows another example of the crossover transition in the f-electron densities of states $\rho_f(\omega)$ from the incoherent to the coherent Kondo-lattice state with temperature for the Kondo regime close to the valence-fluctuation regime. The f-level resonance peaks at ε_f^* merge into the enhanced Kondo-resonance peaks at lower temperatures here. Again, the crossover splitting to the coherent state starts at several T_K ($T_K = 20$ K), and the lower-energy coherent peak grows very sharp, shifting its position from ϵ_F to of order $O(T_K)$ (here ~ 6 K) below ϵ_F, and finally is fixed below the temperature $T_0 \sim 0.1T_K$. The dip continues to become deeper on ϵ_F. Therefore, these features seem to be universal in the Kondo-lattice system, and $T_0 \sim 0.1T_K$ can be defined as the coherence temperature. Here, the width of the sharp coherent peak is of order $O(T_K)$ below the temperature T_0 and causes the heavy-fermion quasiparticle bandwidth to be as wide as $\sim T_K$. However, as we mentioned

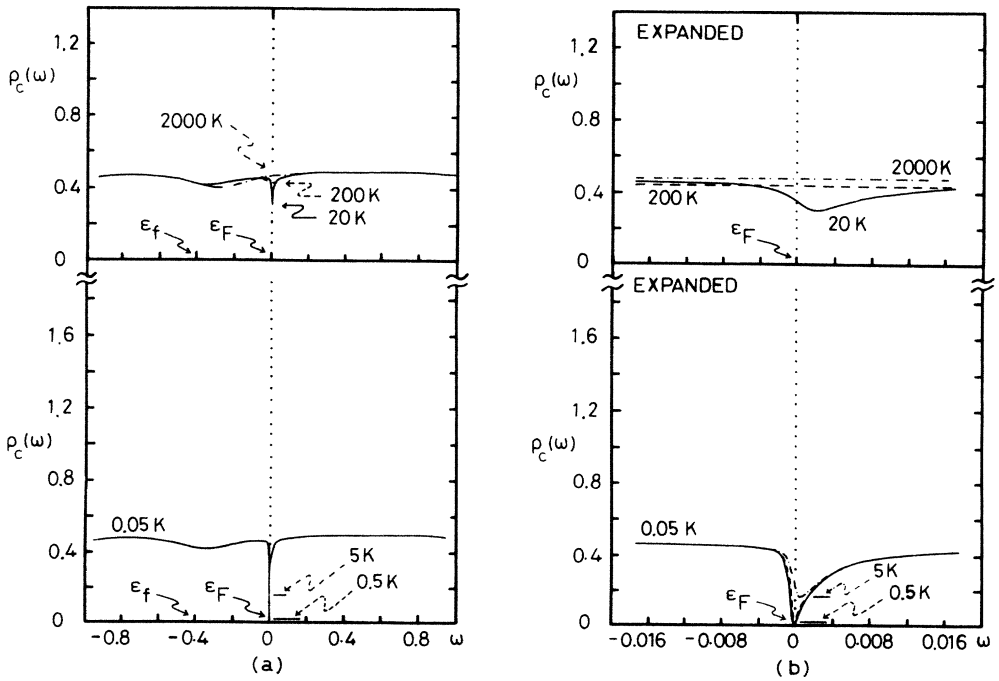

FIG. 3. The density of states $\rho_c(\omega)$ [(a) and expanded (b)] of conduction electrons for the Anderson-lattice model, corresponding to the Kondo regime of Fig. 2 for the same parameters. $\rho = 1/2D = 0.5$ is the unperturbed conduction density of state.

in Sec. III B, this quasiparticle bandwidth itself does not play as the coherence temperature T_0 because it is the maximum temperature above which the quasiparticle state is destroyed.

Next, we study the cases of the valence-fluctuation regime in the behaviors of $\rho_f(\omega)$ and the f-electron number per site n_f with change in temperature. First, we show in Fig. 5 the temperature dependence of $\rho_f(\omega)$ for the case of the bare f-level ε_f placed right on the Fermi level ϵ_F which is kept at zero, $\varepsilon_f=\epsilon_F=0$ [in which case $\varepsilon_f^*=\varepsilon_f$ in Eq. (27)] without fixing the total electron number $n=n_f+n_c$. It is seen that with decrease in temperature the renormalized f-level $\varepsilon_f^{**}(T)$, whose renormalization still comes from $F(\omega)$, Eq. (23), at the position of the hybridization dip moves above ϵ_F, being settled at the energy given

$$\varepsilon_f^{**}(0)-\epsilon_F=(\Delta/\pi)\ln[D/(\varepsilon_f^{**}(0)-\epsilon_F)]$$

as $T\to 0$, and the enhanced double-peak resonance appears. The hybridization dip at $\varepsilon_f^{**}(T)$ tends to saturate in depth for $T\to 0$. Above the temperature $T\sim\varepsilon_f^{**}(0)-\epsilon_F$ the renormalized level $\varepsilon_f^{**}(T)$ shifts and the electron numbers n_f and n decrease but they do not change below it (in this case ~ 200 K).

If for decreasing temperature the chemical potential μ is adjusted self-consistently so as to keep the constant total electron number n, then the valence-fluctuation spectra as shown in Fig. 6 are obtained. The amount of the shift of μ approximately corresponds to the shift $[\varepsilon_f^{**}(T)-\epsilon_F]$ of the dip of Fig. 5 (as if the shifted chemical potential μ came to the dip), but instead of the dip a very large f-resonance peak tends to sit on the new chemical potential. It is remarkable that when the nonhybridized bare f-level ε_f is placed just on the Fermi level ϵ_F ($\varepsilon_f=\epsilon_F$), as is the case of the valence-fluctuation situation, then to keep the same total electron number n with decrease in temperature, the shifted chemical potential μ is always pinned down on the large

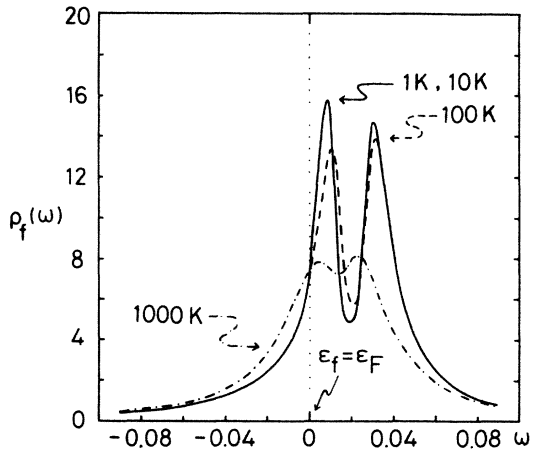

FIG. 5. Temperature-dependent $\rho_f(\omega)$ of the Anderson-lattice model in the valence-fluctuation regime ($\varepsilon_f=\epsilon_F$) for the fixed Fermi level ($\epsilon_F=0$) without fixing the total number of electrons, $n=n_f+n_c$. $V=0.1$, $U=\infty$, $\pi\Delta=0.05$, and $D=1$. $n_f=0.38$ for $T\leq 10$ K and $n_f=0.45$ for $T=100$ K, and $n_f=0.64$ for $T=1000$ K.

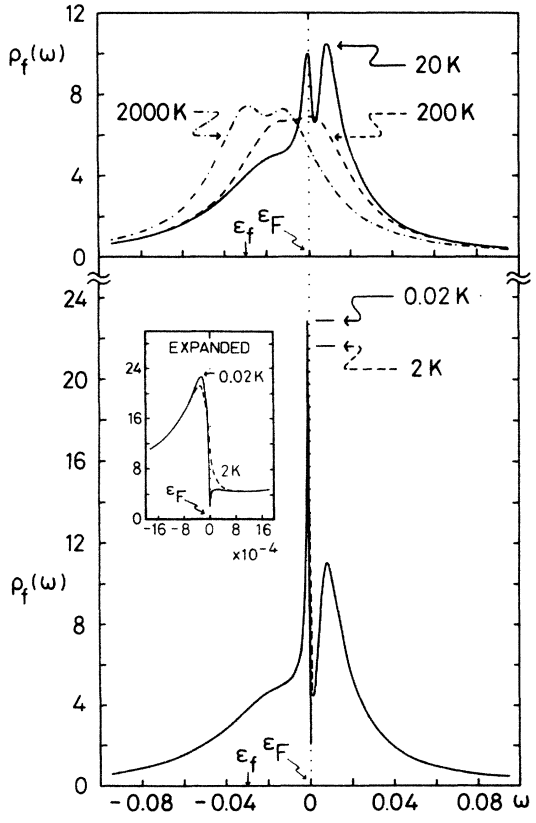

FIG. 4. Another case of the crossover behavior of $\rho_f(\omega)$ for the Anderson-lattice model in the Kondo regime close to the valence-fluctuation regime. $T_K=20$ K, $\varepsilon_f=-0.03$, $V=0.1$, $U=\infty$, $\pi\Delta=0.05$, $\epsilon_F=0$, and $D=1$. $n_f=0.69$ for $T\leq 200$ K. The temperature dependences of the $\rho_f(\omega)$ structures below $T=0.1T_K$ do not change as in Fig. 2.

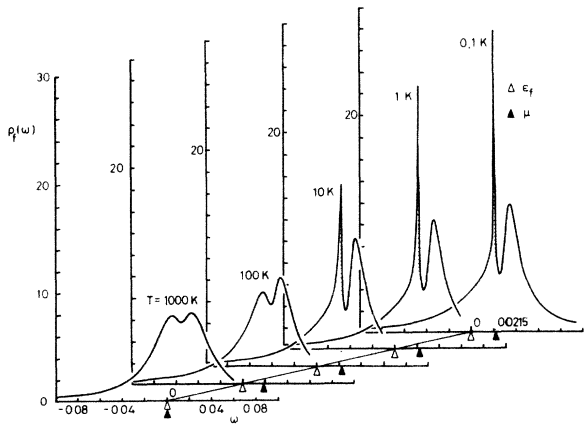

FIG. 6. Valence-fluctuation $\rho_f(\omega)$ for the constant total electron number $n=n_f+n_c$ ($=1.63$) with fixed f-level $\varepsilon_f=0$. The chemical potential μ shifts with decreasing temperature, but stops below $T\sim 10$ K. Notice that the chemical potential μ exactly follows the position of the lower-energy resonance peak: $\mu=0$ for $T=1000$ K ($n_f=0.64$); $\mu=0.0190$ for $T=100$ K ($n_f=0.62$); $\mu=0.0215$ for $T\leq 10$ K ($n_f=0.61$). The other parameters are the same as in Fig. 5.

(and sharp) f-resonance peak obtained in the self-consistent density-of-states solutions.

In Fig. 7 we show the crossover transition from the Kondo-lattice states to the valence-fluctuation states in $\rho_f(\omega)$ with approach of ε_f level to the Fermi level at the constant temperature $T=3.7$ K. As the f-level resonance passes through ϵ_F, the sharp and broad Kondo-lattice peaks are swept away to become the double-peak resonance of the latter states.

V. DISCUSSION

The present Green-function decoupling theory is an approach from the high-temperature regime, where the physical properties of the Anderson-lattice model from the Kondo-lattice regime to the valence-fluctuation regime through the crossover regime are correctly derived in the systematic and unified treatments. The single-site Kondo-resonance phenomenon has been extensively studied in the decoupling[22,23] and other[35,38] approximations in the impurity Anderson model; however, we are not yet familiar with how the lattice Kondo resonances arises in the Anderson-lattice model.[17,19] Therefore, it was our main purpose to study how the coherent Kondo-resonance phenomenon shows up in the Kondo-lattice system of the Anderson-lattice model, in particular in relation to the heavy-fermion quasiparticle states. It is quite interesting to find, as we have seen, that the incoherent Kondo resonances at individual sites begin to crossover to the coherent Kondo state above the impurity Kondo temperature T_K, and the coherence in the Kondo lattice is fully developed at the temperature $\sim 0.1T_K$. This crossover behavior exhibits the difference between the lattice and the impurity Kondo effects. The crossover transitions from the Kondo-lattice states to the valence-fluctuation states with the f-level ε_f approaching the Fermi level ϵ_F reveals the range of the appearance of the lattice Kondo states and the relation between the valence-fluctuation spectra and the Kondo-lattice spectra.

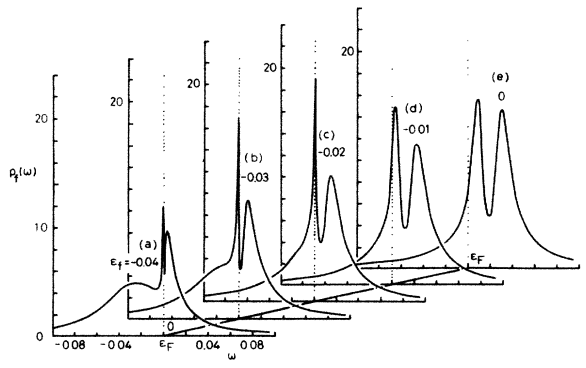

FIG. 7. Crossover transition from the Kondo-lattice states to the valence-fluctuation states for the constant temperature $T=3.7$ K with the movement of the f-level ε_f: (a) $\varepsilon_f=-0.04$, $n_f=0.75$, $T_K=3.7$ K; (b) $\varepsilon_f=-0.03$, $n_f=0.68$, $T_K=20$ K; (c) $\varepsilon_f=-0.02$, $n_f=0.60$; (d) $\varepsilon_f=-0.01$, $n_f=0.49$; (e) $\varepsilon_f=0$, $n_f=0.38$. The lower-energy Kondo peak near ϵ_F becomes the maximum when it falls exactly on ϵ_F in the critical situation between the Kondo and the valence-fluctuation regimes. $V=0.1$, $U=\infty$, $\pi\Delta=0.05$, $\epsilon_F=0$, and $D=1$.

If we write the Green function of Eq. (18) as

$$\langle\langle f_{\mathbf{k},\sigma}, f^{\dagger}_{\mathbf{k},\sigma}\rangle\rangle = \frac{1}{\omega-\varepsilon_f-\Sigma(\omega)-\dfrac{V^2}{\omega-\varepsilon_{\mathbf{k}}}} , \tag{50}$$

then the self-energy $\Sigma(\omega)$ is written as

$$\Sigma(\omega)=\frac{1}{A(\omega)}\{B(\omega)+[A(\omega)-1](\omega-\varepsilon_f)\} . \tag{51}$$

An advantage of this high-temperature approach is to be able to show easily that near the impurity Kondo temperature T_K this self-energy $\Sigma(\omega)$ exhibits the logarithmic Kondo resonance and its derivative $1-\partial\Sigma(\omega)/\partial\omega$ gives the large renormalization of the hybridization from V to $\tilde{V}\sim T_K^{1/2}$, respectively. We have seen through the Green functions in Sec. II C that this self-energy $\Sigma(\omega)$ is different from the self-energy $\Sigma_{\text{imp}}(\omega)$ of the single-site approximation or the impurity system. The imaginary part of the lattice self-energy $\Sigma(\omega)$ is much smaller than that of the impurity self-energy in the wider region around the Fermi energy. The quasiparticle renormalization factor $1-\partial\Sigma(\omega)/\partial\omega$ is smaller in the lattice case than in the impurity case.

A comparison of Figs. 1 and 2 reveals that the lattice Kondo states deviate from the impurity Kondo states below the temperature of several T_K, where coherence has begun to be introduced, although the former incoherent Kondo resonance is very similar to the impurity one above that temperature. The essential differences between the lattice and impurity Kondo states at the low temperatures are that (i) the sharp and larger low-energy peak comes of order T_K below ϵ_F in the former, while the broader Kondo peak tends to the Fermi level ϵ_F from above as $T\to 0$ in the latter, (ii) the temperature dependence of the lattice Kondo resonance stops below $\sim 0.1T_K$, and (iii) there exists a very sharp pseudogap on the Fermi level in the Kondo lattice state where $\rho_f(\epsilon_F)\to 0$ as $T\to 0$. However, if the quasiparticle densities of states are constructed from the lattice Kondo-resonance peak, the renormalized huge quasiparticle spectrum of the width $\sim O(T_K)$ has a finite density of states without a pseudogap at ϵ_F, and tends to be fixed below $T_0\sim 0.1T_K$. Thus, the Kondo-lattice system is expected to exhibit the strong temperature-dependent properties in the crossover regime, several $T_K \gtrsim T \gtrsim T_0$ ($\sim 0.1T_K$), which is different from those in the incoherent Kondo regime at higher temperatures, and the weak temperature-dependent properties in the heavy-fermion quasiparticle regime, $T \lesssim T_0$.

These remarkable differences lead to the results which are consistent with the recent experimental observations[9,13–15] that in the heavy-fermion Kondo-lattice systems there is a maximum $\gamma_{\max}$ in the temperature dependence of the enhanced specific-heat coefficient $\gamma(T)$ below T_K, whereas in the impurity Kondo systems or the Kondo alloys the $\gamma(T)$ shows a monotonous increase.[13] Furthermore, the experimental data for the $\gamma(T)$ of the Kondo lattice $CeAl_3$ obtained by Andres *et*

al.[9] and Bredl *et al.*[13] [and probably for $CeCu_2Si_2$ (Ref. 13) and $CeCu_6$ (Ref. 15) also] show that the $\gamma(T)$ approaches some constant value after decreasing from the maximum γ_{max} as T tends to 0 K. The low-temperature behaviors of the coherent Kondo resonance in Figs. 2 and 4 suggest that as temperature is decreased, there are several competing factors for the quasiparticle contributions to the specific-heat coefficient $\gamma(T)$, resulting in a maximum γ_{max} in the crossover region: the growth and the shift of the lower-energy coherent peak, the initial development of the rather wide pseudogap, the thermal excitation comparable to the peak width, and the somewhat growing quasiparticle renormalization factor. Near the temperature $T_0 \sim 0.1 T_K$ the whole f-electron spectrum has been fixed except only the sharp pseudogap on ϵ_F becoming deeper. Since the source of the quasiparticle spectrum comes entirely from the sharp coherent peak of the f electron, and there is no quasiparticle spectrum in the pseudogap, the quasiparticle spectrum is also locked near this temperature. We have recently studied the temperature-dependent quasiparticle densities of states based on the results of the present study and have obtained the specific-heat coefficient $\gamma(T)$ as a function of temperature. According to this study the origin of the appearance of γ_{max} and the subsequent decrease to a constant value can be interpreted along the lines explained above. The details of this investigation will be described in a separate paper.

The existence of a gaplike structure in the periodic Kondo resonance was first suggested by Martin.[16] The temperature-dependent f-electron spectra have been studied in the Kondo-lattice system of the Anderson model by Grewe,[17] who has first demonstrated by numerical calculation that the Kondo-lattice state gives rise to a splitting in the Kondo-resonance peak with a pseudogap being developed for temperatures $T \ll T_K'$ [his T_K corresponds to T_K' in Eq. (44) here]. Although there is similarity in the position of the low-energy peak to the present result, the width of the pseudogap is $\sim T_K'/4$ wide and the higher-energy peak is not as broad as ours. Koyama and Tachiki[19] have recently obtained the f-electron densities of states near the Fermi level at finite temperatures for the Kondo regime in the one-loop approximation of spin fluctuation. They found the sharp lower-energy peak centered on ϵ_F and the broad resonance peak at a higher energy, and observed that the narrow peak responsible for the heavy-fermion states decays easily to the single-impurity-like incoherent Kondo resonance states with a small temperature increase. This latter result is very similar to the present one, but the significant discrepancy is the position of the sharp lower-energy and the absence of a clear pseudogap.

We have seen in Fig. 6 that for the typical situation of the rare-earth valence-fluctuation systems where the nonhybridized f-level ε_f is just on the Fermi level, the shifted chemical potential μ is always pinned on the Kondo-like sharp f-resonance peak. This f resonance peak on the chemical potential becomes very sharp by fast charge and spin fluctuations at low temperatures. However, the parameter situations which more closely resemble the collapsed metallic SmS with a pseudogap and the semiconducting SmB_6 with a small real gap would be rather close to the Kondo-regime parameters of Fig. 4.

[1] P. A. Lee, T. M. Rice, J. W. Serene, L. J. Sham, and J. W. Wilkins, Comments Condensed Matter Phys. **12**, 99 (1986).

[2] G. R. Stewart, Rev. Mod. Phys. **56**, 755 (1984).

[3] P. Coleman, Phys. Rev. B **28**, 5255 (1983).

[4] N. Read, D. M. Newns, and S. Doniach, Phys. Rev. B **30**, 3841 (1984).

[5] P. W. Anderson, Phys. Rev. B **30**, 1549 (1984).

[6] F. Steglich, J. Aarts, C. D. Bredl, W. Lieke, D. Meshede, W. Franz, and J. Schäfer, Phys. Rev. Lett. **43**, 1892 (1979).

[7] H. R. Ott, H. Rudigier, Z. Fisk, and J. L. Smith, Phys. Rev. Lett. **50**, 1595 (1983).

[8] G. R. Stewart, Z. Fisk, J. O. Willis, and J. L. Smith, Phys. Rev. Lett. **52**, 679 (1984).

[9] K. Andres, J. E. Graebner, and H. R. Ott, Phys. Rev. Lett. **35**, 1779 (1975).

[10] H. R. Ott, H. Rudigier, Z. Fisk, and J. L. Smith, Physica B&C **127B**, 359 (1984).

[11] W. Lieke, U. Rauchschwalbe, C. D. Bredl, F. Steglich, J. Aarts, and F. R. de Boer, J. Appl. Phys. **53**, 2111 (1982); F. Steglich, C. D. Bredl, W. Lieke, U. Rauchschwalbe, and G. Sparn, Physica B&C **126B**, 82 (1984).

[12] A. Sumiyama, Y. Oda, H. Nagano, Y. Onuki, and T. Komatsubara, J. Phys. Soc. Jpn. **54**, 877 (1985); Y. Onuki, Y. Shimizu, M. Nishihara, Y. Machii, and T. Komatsubara, *ibid.* **54**, 1964 (1985); **54**, 2804 (1985).

[13] C. d. Bredl, S. Horn, F. Steglich, B. Lüthi, and R. M. Martin, Phys. Rev. Lett. **52**, 1982 (1984).

[14] G. E. Brodale, R. A. Fisher, C. M. Lisse, N. E. Phillips, and A. S. Edelstein, J. Magn. Magn. Mater. **54-57**, 416 (1986).

[15] T. Fujita, K. Satoh, Y. Onuki, and T. Komatsubara, J. Magn. Magn. Mater. **47-48**, 66 (1985).

[16] R. M. Martin, Phys. Rev. Lett. **48**, 362 (1982).

[17] N. Grewe, Solid State Commun. **50**, 19 (1984).

[18] C. Lacroix, J. Magn. Magn. Mater. **60**, 145 (1986); C. Lacroix, J. Magn. Magn. Mater. **63&64**, 239 (1987).

[19] T. Koyama and M. Tachiki, Phys. Rev. B **36**, 437 (1987); T. Koyama and M. Tachiki, Phys. Rev. B **34**, 3272 (1986).

[20] E. Abrahams and C. M. Varma, in *The Theory of the Fluctuating Valence State,* edited by T. Kasuya (Springer-Verlag, New York, 1985).

[21] B. A. Jones and C. M. Varma, Phys. Rev. Lett. **58**, 843 (1987).

[22] A. Theumann, Phys. Rev. **178**, 978 (1969).

[23] C. Lacroix, J. Phys. F **11**, 2389 (1981).

[24] Y. Nagaoka, Phys. Rev. **138**, A1112 (1965).

[25] G. Czycholl, Phys. Rev. B **31**, 2867 (1985).

[26] A. J. Fedro and S. K. Sinha, in *Valence Instabilities,* edited by P. Wachter and H. Boppart (North-Holland, Amsterdam, 1982) p. 371.

[27] T. Costi, J. Magn. Magn. Mater. **47-48**, 384 (1985).

[28]H. G. Baumgärtel and E. Müller-Hartmann, in *Valence Instabilities,* Ref. 26, p. 57.
[29]Z. Tesanovic and O. T. Valls, Phys. Rev. B **34**, 1918 (1986).
[30]M. Lavagna, A. J. Millis, and P. A. Lee, Phys. Rev. Lett. **58**, 266 (1987).
[31]Assa Auerbach and K. Levin, Phys. Rev. Lett. **57**, 877 (1986).
[32]A. Yoshimori and H. Kasai, J. Magn. Magn. Mater. **31**, 475 (1983).
[33]M. Tachiki and S. Maekawa, Phys. Rev. B **29**, 2497 (1984).
[34]P. W. Anderson, Phys. Rev. **126**, 41 (1961).
[35]O. Gunnarsson and K. Schönhammer, Phys. Rev. B **28**, 4315 (1983).
[36]T. M. Rice and K. Ueda, Phys. Rev. Lett. **55**, 995 (1985).
[37]H. Kaga and Y. Shibuya, J. Phys. C **17**, 2313 (1984).
[38]H. Kojima, Y. Kuramoto, and M. Tachiki, Z. Phys. B **54**, 293 (1984).